THE JOURNAL OF BIOLOGICAL CHEMISTRY
Vol. 276, No. 37, Issue of September 14, pp. 34853–34861, 2001

Printed in U.S.A.

The Neurokinin A Receptor Activates Calcium and cAMP Responses through Distinct Conformational States*

Received for publication, May 14, 2001, and in revised form, July 17, 2001
Published, JBC Papers in Press, July 17, 2001, DOI 10.1074/jbc.M104363200

Tania Palanche‡§, Brigitte Ilien‡§, Sannah Zoffmann‡§, Marie-Pierre Reck‡§, Bernard Bucher§¶, Stuart J. Edelstein‖, and Jean-Luc Galzi‡§**

From ‡CNRS UPR 9050, Ecole Supérieure de Biotechnologie de Strasbourg, Boulevard Sébastien Brant, 67400 Illkirch, France, ¶Pharmacologie et Physico-Chimie des Interactions Cellulaires et Moléculaires, Faculté de Pharmacie 74, Route du Rhin, BP 24 67401 Illkirch, France, §Institut Fédératif de Recherche IFR 85 et FR 2059, 67400 Illkirch, France, and the ‖Department of Biochemistry, 30 Quai Ernest-Ansermet, CH-1211 Geneva 4, Switzerland

G protein-coupled receptors are thought to mediate agonist-evoked signal transduction by interconverting between discrete conformational states endowed with different pharmacological and functional properties. In order to address the question of multiple receptor states, we monitored rapid kinetics of fluorescent neurokinin A (NKA) binding to tachykinin NK2 receptors, in parallel with intracellular calcium, using rapid mixing equipment connected to real time fluorescence detection. Cyclic AMP accumulation responses were also monitored. The naturally truncated version of neurokinin A (NKA-(4–10)) binds to the receptor with a single rapid phase and evokes only calcium responses. In contrast, full-length NKA binding exhibits both a rapid phase that correlates with calcium responses and a slow phase that correlates with cAMP accumulation. Furthermore, activators (phorbol esters and forskolin) and inhibitors (Ro 31-8220 and H89) of protein kinase C or A, respectively, exhibit differential effects on NKA binding and associated responses; activated protein kinase C facilitates a switch between calcium and cAMP responses, whereas activation of protein kinase A diminishes cAMP responses. NK2 receptors thus adopt multiple activatable, active, and desensitized conformations with low, intermediate, or high affinities and with distinct signaling specificities.

Signaling by G protein-coupled receptors takes place through transient interactions between different proteins, the receptor, GTP-binding proteins, and effector enzymes or channels. Each interaction constitutes potential branching for multiple response pathways with different time courses, targets, and regulatory processes (1–7). Depending on the activated signaling pathway, cell responsiveness has been shown to be regulated at the level of the receptor itself and/or at the level of one of the intracellular effectors. For example, G_q-mediated intracellular calcium release declines as a result of IP_3[1] receptor inactivation (8). Concomitantly, the receptor can be subject directly to short or long term regulations that play determinant roles in the control of olfaction, vision, or neurotransmission in mammals (9), for example. The most prevalent mechanisms for short term regulation of G protein-coupled receptors involve their phosphorylation by G protein-coupled receptor protein kinases or second messenger-dependent protein kinases such as protein kinases A (PKA) or C (PKC). Such regulation, which generally leads to termination of one signaling pathway, may turn on alternative intracellular responses (G_s to G_i). Subsequent interactions of the phosphorylated receptors with arrestins constitute the initial step for receptor internalization through clathrin-coated pits and also lead to scaffolding complexes that activate the mitogen-activated protein (MAP) kinase cascade (2, 3).

The possibility that receptors exist in multiple active states is documented by a growing body of experimental evidence. Distinct agonists of opioid receptors differentially stimulate receptor phosphorylation and endocytosis (10); cholecystokinin receptor antagonists lead to receptor internalization without promoting its phosphorylation (11); and phosphorylation of the angiotensin receptor occurs in a conformation that differs from the active state (12). Although theoretical descriptions of G protein-coupled receptors within a framework of multiple conformational states have been reported (13), very few experimental approaches were developed to address this issue in dynamic terms.

Tachykinins (substance P, neurokinin A (NKA), and neurokinin B) act as neurotransmitters in the enteric nervous system (14, 15), spinal cord, and brain (16–18). They exhibit preferential binding to three receptor subtypes, NK1, NK2, and NK3, respectively. Stimulation of these receptors by selective agonists leads to multiple intracellular events such as elevation of intracellular calcium concentration through phospholipase C activation, stimulation of cyclic AMP formation, activation of the MAP kinase cascade, or stimulation of phospholipases (3, 19–22) with different sensitivities toward distinct agonist molecules.

In a previous report (23), we have described a fluorescent NK2 receptor labeled with enhanced green fluorescent protein (EGFP) that allows simultaneous real time recording of ligand binding and calcium responses to be carried out in living cells. We showed that two natural agonists, NKA and its truncated form, NKA-(4–10) (24), differed in that NKA triggers rapidly desensitizing calcium responses, whereas repetitive NKA-(4–10) administration did not alter cell responsiveness (23, 25), supporting the conclusion that at least part of response desen-

* This work was supported by CNRS, INSERM, the Association pour la Recherche sur le Cancer, the Fondation pour la Recherche Médicale, the Ligue Nationale Contre le Cancer (Comité du Haut-Rhin), the Agence Nationale pour la Recherche sur le SIDA, the Université Louis Pasteur de Strasbourg, and SIDACTION (to T. P.). The costs of publication of this article were defrayed in part by the payment of page charges. This article must therefore be hereby marked "*advertisement*" in accordance with 18 U.S.C. Section 1734 solely to indicate this fact.

** To whom correspondence should be addressed. Tel.: 33-3-90-24-47-59; Fax: 33-3-90-24-48-29; E-mail: galzi@esbs.u-strasbg.fr.

[1] The abbreviations used are: IP_3, inositol 1,4,5-trisphosphate; NKA, neurokinin A; PMA, phorbol 12-myristate 13-acetate; PKC, protein kinase C; PKA, protein kinase A; H89, *N*-[2((*p*-bromocinnamyl)amino)-ethyl]-5-isoquinolinesulfonamide; TR, Texas Red; MAP, mitogen-activated protein; EGFP, enhanced green fluorescent protein; BAPTA, 1,2-bis(2-aminophenoxy)ethane-*N*,*N*,*N*′,*N*′-tetraacetic acid.

sitization to NKA was due to lack of receptor responsiveness.

In this study, we further analyze the action of the two agonist peptides, NKA and NKA-(4–10), fluorescently labeled with Texas Red. Monitoring ligand binding kinetics, time-resolved agonist-evoked calcium and cAMP responses, and sensitivity of binding and responses to protein kinase activators and inhibitors support a multistate receptor model with differential stabilization of discrete conformations of the receptor by NKA and NKA-(4–10).

EXPERIMENTAL PROCEDURES

Synthesis of Fluorescent NKA Analogs—Two peptides, NKA (HKTDSFVGLM-NH_2) and a cysteine-containing analog of NKA-(4–10) (DSFCGLM-NH_2), were derivatized with iodoacetyl-C^5-Texas Red, purified as described (23), and characterized as the mono-Texas Red derivative of neurokinin A (labeled on the N terminus and designated as TR1-NKA) or of neurokinin A-(4–10) (labeled at residue Cys-4 and designated as TR7-NKA-(4–10)) by spectrofluorometry and by matrix-assisted laser desorption ionization/time of flight-mass spectrometry (calculated molecular mass, 1865.3 daltons; determined as 1865.5 for TR1-NKA; calculated molecular mass, 1501.7 daltons; determined as 1501.8 for TR7-NKA-(4–10)).

Preparation of HEK 293 cells expressing the EGFP-labeled fluorescent NK2 receptor and radioligand binding assays using [^{3}H]SR 48968 were as described (23).

Fluorescence Measurements—Fluorescence measurements from cell suspensions were made as described (23) in Hepes buffer (in mM: 137.5 NaCl, 1.25 $MgCl_2$, 1.25 $CaCl_2$, 6 KCl, 5.6 glucose, 10 Hepes, 0.4 NaH_2PO_4, 1% bovine serum albumin (w/v), pH 7.4) supplemented with protease inhibitors (bestatin, aprotinin, phosphoramidon, chymostatin, and leupeptin).

Stopped-flow Experiments—Rapid kinetic experiments were carried out with an Applied Photophysics SK1E rapid mixing apparatus modified for rapid and non-damaging mixing of living cells. The valves located at syringe output were modified to allow linear liquid flow in a 2-mm internal diameter tubing that progressively decreased to 1 mm internal diameter. The mixing chamber was composed of a 1-mm internal diameter T-shaped Teflon connector. The observation chamber was a Hellma 176.002 (100 μl) quartz circulation cuvette placed on the cuvette holder of the SPEX fluorolog 2 spectrofluorometer. Fluorescence measurements were carried out in the photon counting mode (integration times 1–100 ms depending on ligand concentration) and were corrected for light flux variations with a reference photomultiplier measuring rhodamine fluorescence. All measurements were made at 21 °C. At a typical 12 bar air ram pressure the flow rate was 4 ± 0.5 ml/s. Cell counting before and after mixing indicated that less than 5% of the cells were damaged. Each measurement started after renewal of 7–8 times the volume of the observation cuvette. The dead volume (100 μl) and dead time of the apparatus (25 ± 5 ms) were experimentally determined. Such configuration of the mixing device typically allows measurement of fluorescence relaxations with apparent rate constants up to 10 s^{-1}.

Data were stored using the DM3000 software provided with the spectrofluorometer and analyzed with Kaleidagraph (Synergy Software) by various analytical expressions such as exponentials, sum of exponentials, or sum of exponentials and linear relationships (26). Each relaxation process was characterized by the values of its amplitude and of its rate constant k_{app}. The uniqueness of the fit was checked by repeated calculations performed with distinct experimental data points (from several experiments) or with distinct values for the initiation of the fitting procedure. Some variations among different cell batches were noted but within modest limits.

Linear k_{app} *versus* [ligand] relationships were analyzed according to a bimolecular interaction Scheme 1,

$$R + L \leftrightarrow RL$$

SCHEME 1

and fitted using the corresponding Equation 1,

$$k_{app} = k_1 \times L + k_{-1} \quad \text{(Eq. 1)}$$

where k_1, the slope of the line, is the association rate constant, and k_{-1}, the intercept with the ordinate, is the dissociation rate constant.

Non-linear k_{app} *versus* [ligand] relationships were analyzed according to Scheme 2 comprising a bimolecular interaction followed by the interconversion to a second conformation,

$$R + L \leftrightarrow RL \leftrightarrow R'L$$

SCHEME 2

and were fitted using the corresponding expression in Equation 2,

$$k_{app} = k_2 \times (L/(L + K_D)) + k_{-2} \quad \text{(Eq. 2)}$$

where K_D is the dissociation constant for the formation of the *RL* complex, and k_2 is the forward and k_{-2} the backward rate constant of the equilibration between *RL* and *R′L*.

Calcium Response Analysis—Intracellular calcium elevation was recorded in triplicate with the rapid mixing apparatus, using indo-1 as the fluorescent probe and analyzed as described (27). Comparison with binding was carried out on data obtained on the same day using unique cell and ligand batches.

Inositol Triphosphate Determination—After preincubation for 15 min at 22 °C in the absence or presence of various agents (10 mM LiCl being systematically added during the last 5 min of preincubation), cells (2×10^6 cells per assay) were challenged for 30 s at 22 °C in the absence (basal level) or the presence of agonist. IP_3 content was determined using a [^{3}H]IP_3 radioreceptor assay kit (PerkinElmer Life Sciences).

cAMP Measurements—Receptor coupling to adenylyl cyclase was determined in 24-well plates as described (28).

Ligand Binding Modeling—Experimental binding curves were fit with either a two- or a three-state allosteric model as described (29). The theoretical model simulates ligand binding for a protein with 1–5 ligand-binding sites and 1–4 conformational states in a hierarchical cascade based on increasing affinity for ligand. The conformational states are in freely interconverting equilibria, such that all states are present in defined proportions in the absence of ligand, and their equilibria shift as a function of the kinetics of ligand binding. Each state is characterized by intrinsic ligand binding on- and off-rates and by interconversion rates between neighboring conformational states in the hierarchy that vary with site occupancy according to linear free energy relations. For any set of parameters, the differential equations for ligand binding are solved in the MATLAB computing environment using a program called STOIC.

Chemicals—Synthetic peptides were obtained from Bachem or Neosystem. Forskolin, protein kinase activators and inhibitors, and protease inhibitors were obtained from Sigma and Calbiochem. Fluorescent labels and ion chelators were from Molecular Probes. [^{3}H]SR 48968 was purchased from Amersham Pharmacia Biotech.

RESULTS

Fluorescence Monitoring of the Interactions of TR1-NKA and TR7-NKA-(4–10) with Cells Expressing the EGFP-NK2 Receptor

The two natural peptide agonists, NKA and NKA-(4–10), have been fluorescently labeled with Texas Red. The fluorescent NKA labeled at position 1 is referred to as TR1-NKA. NKA-(4–10) is labeled at position 4 (*i.e.* position 7 of full-length NKA) after substitution of a glycine by a cysteine residue to yield the fluorescent compound hereafter referred to as TR7-NKA-(4–10).

TR1-NKA and TR7-NKA-(4–10) both activate intracellular calcium responses upon interacting with the fluorescent NK2 receptor expressed in HEK 293 cells (Figs. 1*D* and 2*D*). As in the case of their underivatized congeners, they trigger unique (TR1-NKA) or repetitive (TR7-NKA-(4–10)) responses when applied to cells as short pulses of 1 μM solutions (data not shown). In equilibrium binding experiments on cells, they displace the antagonist [^{3}H]SR 48968 with apparent inhibition constants (TR1-NKA, K_I = 100 ± 15 nM; TR7-NKA-(4–10), K_I = 540 ± 170 nM), about 2-fold higher than those of unlabeled NKA (K_I = 60 nM) and NKA-(4–10) (290 ± 65 nM).

The interaction of the two fluorescent peptides with the cell surface-expressed fluorescent NK2 receptor, when followed on a spectrofluorometer with excitation set at 470 ± 10 nm, is monitored as a decrease of EGFP emission at 510 nm due to fluorescence resonance energy transfer. This decrease of EGFP fluorescence is rapid (in the time range of seconds) with TR7-NKA-(4–10) (Fig. 1*A*) and exhibits fast (seconds) and slow (in the time range of minutes) components with TR1-NKA (Fig.

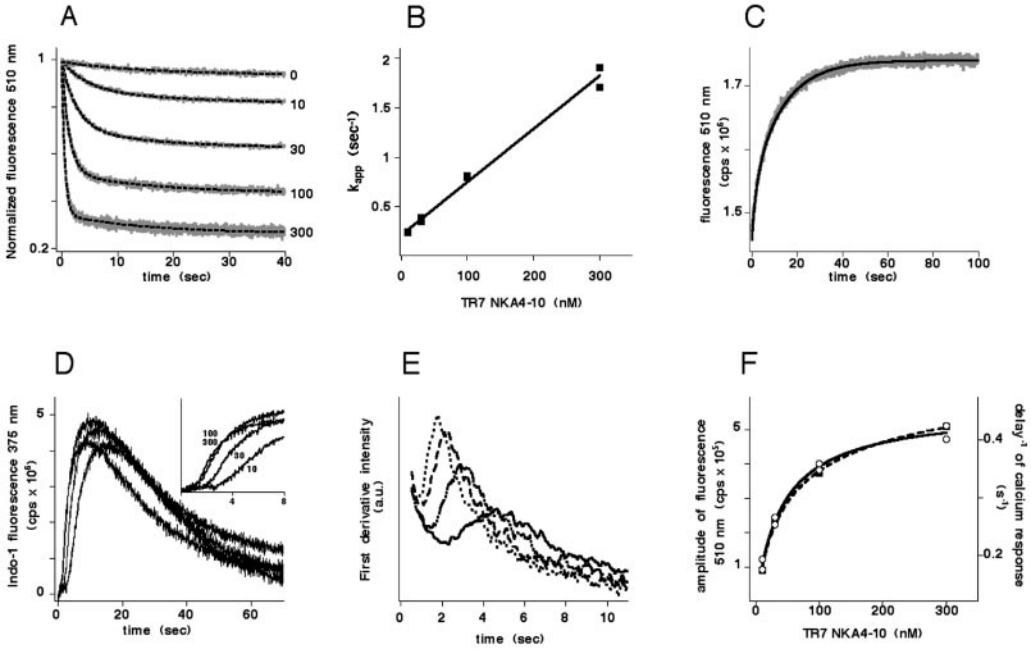

FIG. 1. **Real time recordings of TR7-NKA-(4–10) binding and associated calcium response.** A suspension of 2×10^6 cells/ml is rapidly mixed with buffer containing the desired fluorescent agonist concentration. *A,* time course of TR7-NKA-(4–10) binding to EGFP-NK2R. Each trace corresponds to the mean of three consecutive recordings carried out at the indicated ligand concentrations (nM) at 21 °C. The interaction of saturating concentrations (1–3 μM) of fluorescent agonist results in 15–20% reduction of total sample fluorescence. Data points were acquired every 50 (0–50 nM), 20 (50–300 nM) or 10 ms (beyond 300 nM). Extinction of EGFP fluorescence at 510 nm (excitation 470 nm) is normalized to signal amplitude recorded at 1 μM. The *dotted line* is the best fit with a single exponential decay of fluorescence, taking into account the decay observed in control recordings. *B,* plot of apparent rate constants (k_{app}), determined from fitting binding traces in *A* with a single exponential, *versus* agonist concentration. The slope of the linear regression yields $k_{on} = 5.3 \pm 0.2 \times 10^6$ M^{-1} s^{-1} and $k_{off} \approx 0.21$ s^{-1}. *C,* dissociation of TR7-NKA-(4–10) is initiated by rapid mixing of cells (preincubated at equilibrium with 260 nM ligand) with buffer containing 40 μM SR 48968. The *solid line* is the best fit with two exponentials with k_{off} values of 0.5 ± 0.02 and 0.08 ± 0.004 s^{-1}. *D,* intracellular calcium response recorded in parallel to binding in *A*, using the calcium probe indo-1. Fluorescence in counts/s (*cps*) is recorded at 375 nm (excitation 335 nm). The *inset* represents an 8-s expansion of the response and illustrates variations in response delays. *E,* first derivative of calcium responses shown in *D*. Time to peak corresponds to the time required to reach half-maximal response. *F,* overlap of the amplitudes of TR7-NKA-(4–10) binding determined from fitting data in *A* (*solid line*) with the reciprocal of the response delays measured as the peak of the first derivative of calcium responses in *E* (*dashed line*).

2*A*). At equilibrium, both peptides bind to a saturable number of receptor sites with apparent dissociation constants of $K_D = 9.4 \pm 0.8$ nM (TR1-NKA) and 37 ± 4 nM (TR7-NKA-(4–10)). At temperatures ranging from 10 to 21 °C, 95–100% of the interaction is reversed upon addition of an excess (10–20 μM) of the antagonist SR 48968 or of unlabeled NKA. We also observed previously (23) that in the presence of agonist, fluorescent receptor molecules remain localized to the plasma membrane. Thus, slow processes such as internalization of receptor-ligand complexes are not likely to occur under the conditions of measurements reported here.

Rapid Mixing of a Suspension of Cells Expressing EGFP-NK2R with Texas Red-labeled Peptides

The kinetics of the interaction of TR1-NKA and TR7-NKA-(4–10) with cells expressing EGFP-NK2 receptors were studied using a stopped-flow apparatus modified for cell mixing and equipped for fluorescence recording. Real time agonist binding (Fig. 1*A* and 2*A*) and associated calcium responses (Fig. 1*D* and 2*D*) were recorded in the same experiment, in successive mixings with alternate settings for EGFP or calcium detection.

Quantitative Analysis of TR7-NKA-(4–10) Binding and Associated Responses (Fig. 1)

Ligand Association—Binding traces (Fig. 1*A*) can be analyzed with a single pseudo first-order relaxation (in the time range of seconds) plus a slow exponential drift found in control mixing with ligand-free buffer. This exponential drift, probably due to sedimentation of cells, takes place with a constant rate (0.05 ± 0.005 s^{-1}) at all agonist concentrations. Its amplitude is constant up to 100 nM ligand and progressively increases beyond this concentration but remains within the experimental error for amplitude determination. Binding of TR7-NKA-(4–10) is therefore best described by a single exponential. The apparent rate constant of TR7-NKA-(4–10) can be followed up to the experimental limit of the equipment (2 μM). It increases linearly (Fig. 1*B*) with ligand concentration, with a slope equal to $5.3 \pm 0.2 \times 10^6$ M^{-1} s^{-1} and an intercept with the ordinate at about 0.21 s^{-1}, *i.e.* with a kinetically determined K_D value of about 40 nM. The association rate constant is close to that found for formyl peptide binding to its cognate receptor in neutrophils (30, 31).

The amplitude of the fluorescence signal increases with increasing ligand concentration up to a plateau value around 600 nM. The plot of the amplitudes of EGFP fluorescence as a function of TR7-NKA-(4–10) (Fig. 1*F*) can be fitted with the empirical Hill equation to yield a dissociation constant of 43 ± 8 nM ($n = 3$) and a Hill coefficient of 1.02 ± 0.06, in overall good agreement with equilibrium and kinetic measurement data.

Ligand Dissociation—Dissociation of receptor-ligand complexes, obtained at equilibrium with 260 nM TR7-NKA-(4–10), was initiated by rapid mixing with a large excess (20 μM) of the antagonist SR 48968 (Fig. 1*C*). Identical dissociation relaxations were obtained for preincubation times (association step) lasting from 1 to 10 min. They were not satisfactorily described by a single exponential time course but were best represented using a sum of two exponentials revealing a rapid process ($k_{off} = 0.5 \pm 0.02$ s^{-1}) representing ~40% of the amplitude and a slow ($k_{off} = 0.08 \pm 0.004$ s^{-1}) dissociation step.

Analysis of Calcium Responses—Intracellular calcium re-

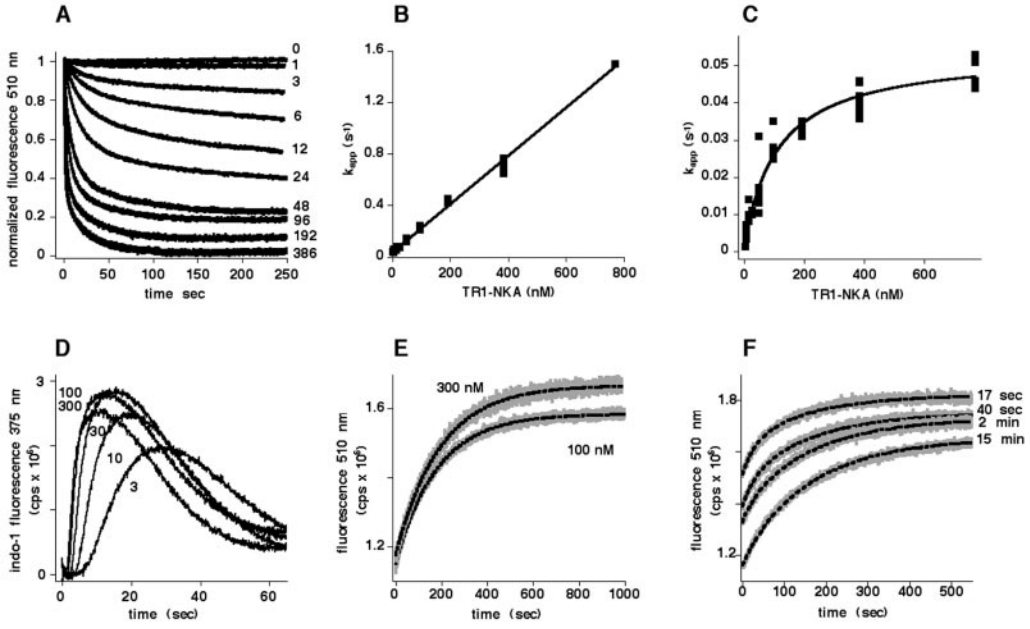

FIG. 2. **Real time recording of TR1-NKA binding and associated calcium response carried out under the same experimental conditions described in the legend to Fig. 1.** *A,* time course of TR1-NKA binding to EGFP-NK2R. The interaction of saturating concentrations of fluorescent agonists results in a 35–50% reduction of total sample fluorescence. Extinction of EGFP fluorescence is normalized to signal amplitude recorded at 1 μM. Each trace is analyzed with a sum of two exponential decays of fluorescence. *B,* plot of apparent rate constants (k_{app}) for the rapid binding relaxation, determined from fitting binding traces in *A* with two exponentials, *versus* agonist concentration. *C,* plot of apparent rate constants (k_{app}) for the slow binding relaxation (determined from fitting binding traces in *A* with two exponentials) *versus* agonist concentration. The *solid line* through the data points is obtained by fitting with Equation 2 under "Experimental Procedures"). *D,* intracellular calcium release recorded on the same day with the same batch of cells as in *A*, with the calcium probe indo-1. *E,* dissociation of TR1-NKA is initiated by rapid mixing of cells (preincubated for at least 20 min with 100 or 300 nM ligand) with buffer containing 20 μM NKA. The *dotted line* is the best fit obtained with a single exponential. *F,* dissociation of TR1-NKA, preincubated for the indicated periods with 50 nM ligand. The *dotted lines* are best fits obtained with two exponentials and relative rapid/slow amplitudes (in percent) equal to 35/65 (17 s), 28/72 (40 s), 15/85 (2 min), and 6/94 (15 min).

sponses (Fig. 1*D*) exhibit maximum amplitudes that are nearly identical within the agonist concentration range that allows significant receptor occupancy to be detected (Fig. 1*A*). In contrast, the delay (time to peak) and the rate at which intracellular calcium concentrations rise follow inverse proportionality with ligand concentration. Responses were therefore analyzed as described by Horn and Marty (27), *i.e.* as the time required to reach half-maximal response using the peak of the first derivative of each response trace (Fig. 1*E*) as a measure of the delay of the response. A plot of the reciprocal of response delays *versus* ligand concentration superimposes with the corresponding amplitude of receptor fluorescence extinction (Fig. 1*F*). The EC_{50} value (≈45 nM) derived from fitting the plot of delays as a function of ligand concentration is in good agreement with TR7-NKA-(4–10) binding affinity. It thus appears that the rate of intracellular calcium elevation correlates with the extent of receptor occupancy.

The experimental data show that association of TR7-NKA-(4–10) with the receptor can be described in terms of a simple bimolecular reaction that is correlated with activation of the calcium response. However, two populations of receptors sites appear to be occupied by the ligand at equilibrium, as reflected by the biphasic ligand dissociation curves.

Quantitative Analysis of TR1-NKA Binding and Associated Responses

Analysis of TR1-NKA binding traces reveals two pseudo-first order relaxation processes that account for more than 95% of the signal and will be referred to as rapid and slow binding steps.

Rapid Binding—This relaxation process develops in the millisecond to second time range (Fig. 2*A*). In agreement with a bimolecular reaction scheme, its apparent rate increases linearly with ligand concentration (Fig. 2*B*), with a slope equal to $2 \pm 0.1 \times 10^6\ M^{-1}\ s^{-1}$, and can be followed up to the limit of the equipment (3 μM). The intercept with the ordinate axis (≈0.04 s^{-1}) gives an estimate of the dissociation rate constant for the rapid relaxation.

The amplitude of the rapid relaxation increases with ligand concentration (Fig. 3*A*) and reaches a plateau above 200 nM. Fitting of the plot of amplitudes *versus* ligand concentration with the empirical Hill equation yields a K_D value of 20 ± 4 nM and a Hill coefficient close to unity (1.07 ± 0.05).

Slow Binding—The slow relaxation process develops in the second to minute time range. The variation of the amplitude of this signal increases with TR1-NKA concentration and reaches a plateau value beyond 100 nM (Fig. 3*B*). Half-maximal amplitude is obtained with ligand concentrations in the 3–4 nM range. The apparent rate constant for this relaxation does not increase linearly with TR1-NKA concentration but tends to reach a plateau value (≈0.05 s^{-1}) at high ligand concentration (Fig. 2*C*). A simple kinetic scheme, involving the binding of TR1-NKA to the receptor, followed by a rate-limiting isomerization toward a higher affinity state, fits the data (Equation 2 under "Experimental Procedures"). The experimental rate constants (k_{app}) can be adequately fit by Equation 2 to give an estimate of the dissociation constant of the initial binding step (best fit obtained with K_D = 190 ± 80 nM), of the intrinsic forward rate of interconversion (k_2 = 0.042 ± 0.09 s^{-1}), and of the backward rate of interconversion (k_{-2} = 0.005 ± 0.002 s^{-1}).

TR1-NKA Dissociation—Dissociation of receptor-ligand complexes obtained at equilibrium (≥20 min) with 100 or 300 nM TR1-NKA was monitored after rapid mixing with excess NKA (10 μM). The dissociation traces obtained are best described by a single exponential relaxation (Fig. 2*E*) with a rate constant (0.0055 ± 0.0002 s^{-1}) indicating that TR1-NKA apparently

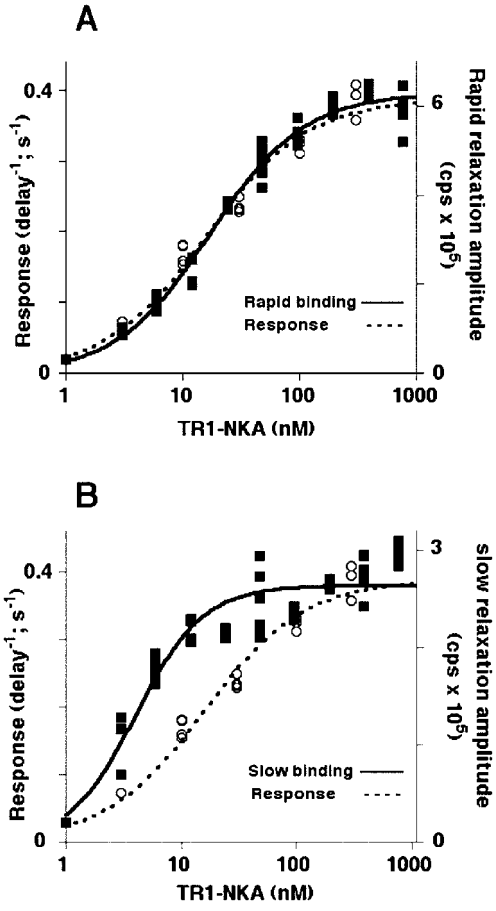

FIG. 3. **Overlap of the amplitudes of TR1-NKA rapid (*A*) and slow (*B*) binding relaxations determined from two exponential fits of data in Fig. 2*A* (*filled squares*) with the reciprocal of response delays of calcium responses in Fig. 2*D* (*open circles*).** Apparent K_D values are 20 nM (rapid binding) and 4 nM (slow binding). EC_{50} of calcium response is equal to 15 nM.

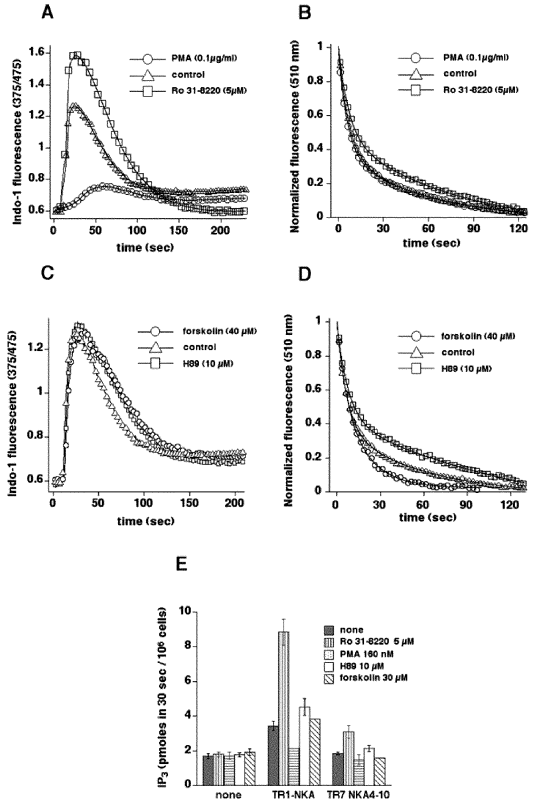

FIG. 4. **Effect of protein kinase activators and inhibitors on TR1-NKA-evoked calcium responses and of TR1-NKA and TR7-NKA-(4–10)-evoked IP_3 formation.** *A* and *C,* TR1-NKA (3 nM) evoked intracellular calcium responses were measured at 21 °C in a fluorescence cuvette equipped with magnetic stirring on the basis of indo-1 375/475 nm ratios, in the presence of 0.1 μg/ml PMA or 5 μM Ro 31-8220 (in *A*) or in the presence of 40 μM forskolin or 10 μM H89 (in *C*) preincubated 10 min before mixing with agonist. *B* and *D,* real time binding of TR1-NKA (50 nM) in the presence of 0.1 μg/ml PMA or 5 μM Ro 31-8220 (in *B*) or in the presence of 40 μM forskolin or 10 μM H89 (in *D*) preincubated 10 min before mixing with agonist. The *solid lines* through data points are best fits obtained with a sum of two exponentials with k_{app} values given in Table I. Traces in *D* are best fit with a constant rapid binding relaxation rate but with different slow binding rates for control, foskolin-, and H89-treated cells. *E,* IP_3 levels (pmol/10^6 cells) are quantified following stimulation of the cells for 30 s with 10 nM TR1-NKA and 50 nM TR7-NKA-(4–10) in the absence or presence of 0.1 μg/ml PMA (160 nM), 5 μM Ro 31-8220, 30 μM forskolin, or 10 μM H89. *Error bars* are standard deviations for at least 3 independent determinations.

occupies a single category of high affinity sites at equilibrium. In contrast, TR1-NKA dissociates faster when preincubation times are shorter (Fig. 2*F*). Dissociation traces obtained after 17- and 40-s and 2- and 15-min incubations of the receptor with 50 nM TR1-NKA are satisfactorily represented with two exponentials comprising a slow step with a rate constant identical to that determined after equilibrium binding (0.0055 ± 0.0002 s^{-1}) and a rapid step with a 6-fold higher apparent rate constant (0.03 ± 0.01 s^{-1}). These two steps exhibit different proportions depending on the time of incubation; after 17 s of binding, rapid dissociation represents more than 30% of total signal amplitude, and after 15 min, it represents less than 10% of the dissociation signal, supporting the hypothesis that stabilization of the receptor in a high affinity state occurs during prolonged exposure to TR1-NKA.

Analysis of Calcium Responses—As noted above with TR7-NKA-(4–10), intracellular calcium responses to TR1-NKA reach maximal amplitudes for partial receptor sites occupancies (Fig. 2*D*). The plot of the reciprocal of response delays *versus* ligand concentration yields an EC_{50} value of ≈15 nM. Superimposition of the rapid binding amplitudes (Fig. 3*A*) or the slow binding amplitudes (Fig. 3*B*) with the reciprocal of response delays clearly illustrates a better correlation between rapid binding and time to half-maximal response.

TR1-NKA thus binds to the NK2 receptor with biphasic kinetics. The rapid binding event correlates with the onset of the calcium response. The slow binding component reflects stabilization of higher affinity sites. In order to further characterize the functional properties of the slow binding component, the effects of activators and inhibitors of protein kinases were studied.

Effects of PKC Activators and Inhibitors on TR1-NKA Binding and Calcium and IP_3 Responses

Intracellular calcium elevation, TR1-NKA binding, and IP_3 formation were determined in the presence of the PKC activator phorbol 12-myristate 13-acetate (PMA) or inhibitor Ro 31-8220. Treatment of cells expressing EGFP-NK2R with PMA leads to a marked reduction in the amplitude of TR1-NKA-evoked intracellular calcium elevation (Fig. 4*A*) and to a smaller but significant decrease in IP_3 formation (Fig. 4*E*). In contrast, these parameters are considerably enhanced in the presence of Ro 31-8220 (Fig. 4, *A* and *E*).

Although PMA attenuates IP_3 and calcium responses, it does not affect the time course of TR1-NKA (50 nM) association to NK2R to a significant extent (Fig. 4*B*). Preincubation of cells with Ro 31-8220 does result in a small retardation in the time

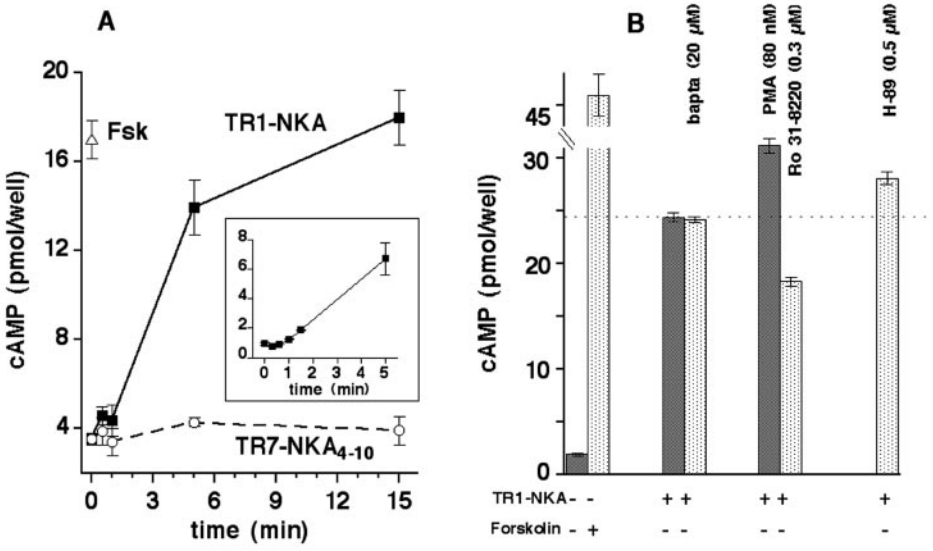

FIG. 5. **cAMP (pmol/well) accumulation in response to 300 nM TR1-NKA or 300 nM TR7-NKA-(4–10).** Response to 30 μM forskolin is shown as a control. *A,* time course of TR1-NKA- and nM TR7-NKA-(4–10)-evoked cAMP accumulation. The *inset* is an independent determination carried out under the same experimental conditions, for which the first 5 min of cAMP accumulation are shown. *B,* effect of protein kinase activators and inhibitors on TR1-NKA-evoked cAMP accumulation. cAMP accumulation was determined after 20 min preincubation with BAPTA-AM, PMA, Ro 31-8220, or H89 at the indicated concentrations, followed by an additional 20-min incubation with 300 nM TR1-NKA. Basal cAMP levels were not significantly changed by the activators and inhibitors of protein kinase C and A. *Error bars* are standard deviation of four independent determinations.

course of TR1-NKA binding (Fig. 4*B*). Kinetic analysis of TR1-NKA binding reveals that neither PMA nor Ro 31-8220 affect the apparent rates for rapid (k_{app} = 0.14 ± 0.01 s^{-1}) and slow (k_{app} = 0.014 ± 0.001 s^{-1}) binding. The effect of Ro 31-8220 is an alteration of the relative amplitudes of rapid *versus* slow binding which change from, respectively, 65/35% (control and PMA) to 50/50% (Ro 31-8220).

Effects of PKA Activators and Inhibitors on TR1-NKA Binding and Calcium and IP_3 Responses

In contrast to PKC modulation, forskolin, which indirectly activates PKA through the stimulation of adenylate cyclase, and the selective PKA inhibitor H89 have slight but not statistically significant effects on TR1-NKA-evoked intracellular calcium elevation (Fig. 4*C*). The two compounds, however, have more pronounced effects on TR1-NKA (50 nM) binding kinetics. As shown in Fig. 4*D,* forskolin accelerates binding, whereas H89 slows it, mainly by changing features of the slow component of TR1-NKA binding. Indeed, neither of the effectors changes the rate of rapid TR1-NKA binding (k_{app} = 0.14 ± 0.01 s^{-1}), but forskolin increases the slow binding rate by about 4-fold (k_{app} = 0.053 ± 0.005 s^{-1}) as compared with control (k_{app} = 0.012 ± 0.002 s^{-1}), and H89 decreases it by about 2-fold (k_{app} = 0.006 ± 0.002 s^{-1}). Moreover, the relative amplitudes of the rapid *versus* slow binding relaxations change from 65/35 for control binding to 55/45 for forskolin-treated and to 45/55 for H89-treated cells.

PKA and PKC effectors have similar effects on IP_3 responses evoked either by TR1-NKA or TR7-NKA-(4–10) (Fig. 4*E*).

Analysis of cAMP Responses

Since effectors of protein kinase A alter TR1-NKA binding, and since NKA is capable of stimulating cAMP formation upon activation of the NK2 receptor (32), we examined the potency of the two fluorescent derivatives, TR1-NKA and TR7-NKA-(4–10), to stimulate cAMP accumulation in cells expressing EGFP-NK2R. As shown in Fig. 5*A*, TR1-NKA (300 nM) produces a marked cAMP elevation, which contrasts with the lack of response to TR7-NKA-(4–10) (up to 1 μM). The TR1-NKA cAMP response takes place with a delay of about 1 min (see *inset*, Fig. 5*A*), becomes detectable at about 1.5 min, and reaches a plateau at about 15–30 min depending on the cell batch. Also, depending on cell batch, the cAMP response evoked by TR1-NKA can be as large as that evoked by 30 μM forskolin (Fig. 5*A*), supporting the notion that adenylate cyclase is activated by TR1-NKA. The TR1-NKA cAMP response is insensitive to calcium chelation by BAPTA, suggesting that cAMP formation is not linked to the elevation of intracellular calcium (Fig. 5*B*). On the other hand, activation of PKC by PMA (80 nM) moderately but significantly increases the amount of cAMP formed after a 15-min stimulation with 300 nM TR1-NKA. Inhibition of PKC and PKA have opposite effects on cAMP formation, as revealed by a depression of the response by Ro 31-8220 (0.3 μM) and a potentiation by H89 (0.5 μM). None of the protein kinase effectors affect basal cAMP levels (data not shown).

DISCUSSION

Results presented here rely on a newly developed rapid fluorescence recording approach to analyze the mode of interaction of two natural agonist neuropeptides that bind in a significantly different manner to the tachykinin NK2 receptor and trigger qualitatively and quantitatively different responses.

NKA binds to the receptor in a two-step process. The rapid binding step correlates temporally with the onset of intracellular calcium elevation and thus reflects, at least in part, stabilization of the receptor in a conformation that activates G proteins. The second binding step with an ~10-fold slower on-rate reflects association of the agonist with a population of sites that arises from the interconversion of a low affinity conformation of the receptor into a higher affinity state. The rate of the slow interconversion reaches saturation at high agonist concentrations. At equilibrium, NKA apparently populates a single category of receptor sites that exhibit high affinity for NKA. Neither the rapid binding nor the slow binding steps are abolished upon activation or inhibition of protein kinases known to phosphorylate the receptor, suggesting that the covalent modifications brought about by phosphorylation of the receptor are not required for the interconversion of the receptor to higher affinity states.

NKA-(4–10) has been isolated as a natural agonist from the fluids of midgut tissue tumors (24). It differs from NKA in that it repetitively activates intracellular calcium release both in oocytes (25) and HEK 293 cells (23) expressing the NK2R, and may be viewed as a "non-desensitizing" agonist with respect to calcium signaling. The fluorescent version of NKA-(4–10) labeled with Texas Red used here, TR7-NKA-(4–10), exhibits an apparent single step association to EGFP-NK2R that temporally correlates with the development of an intracellular calcium response (in the second to minute time range). The slow binding step observed with the long peptide is not detected with

TABLE I
Summary of experimental rate constants
Experimental rate constants of TR1-NKA and TR7-NKA-(4–10) binding to EGFP-NK2R are determined from fluorescence experiments.

Kinetic step	Value of the rate constant	Determination
TR7-NKA-(4–10) ($n = 4$)		
$R\ (0\text{–}1\text{-}2)+L \underset{k_2}{\overset{k_1}{\rightleftharpoons}} R(0\text{–}1\text{-}2)\text{-}L$	$k_1 = 5.3 \pm 0.2 \times 10^6\ M^{-1}\ s^{-1}$	Coefficient of proportionality between k_{app} and TR7-NKA-(4–10) concentration
	$k_2 = 0.21 \pm 0.033\ s^{-1}$	Intercept with the ordinate of the linear k_{app} *versus* TR7-NKA-(4–10) concentration relationship
$R0\text{-}L \xrightarrow{k_3} R0 + L$	$k_3 = 0.5 \pm 0.02\ s^{-1}$	Limiting values of the apparent rate constant for the release of TR7-NKA-(4–10) in the dissociation experiments
$R1\text{-}L \xrightarrow{k_4} R1 + L$	$k_4 = 0.08 \pm 0.004\ s^{-1}$	
TR1-NKA ($n = 4$)		
$R\ (0\text{–}1\text{-}2) + L \underset{k_2}{\overset{k_1}{\rightleftharpoons}} R\ (0\text{–}1\text{-}2)L$	$k_1 = 2 \pm 0.1 \times 10^6\ M^{-1}\ s^{-1}$	Coefficient of proportionality between k_{app} and TR7-NKA-(4–10) concentration
	$k_2 = 0.041 \pm 0.004\ s^{-1}$	Intercept with the ordinate of the linear k_{app} *versus* TR7-NKA-(4–10) concentration relationship
$R0 + L \underset{}{\overset{K_D}{\rightleftharpoons}} R0\text{-}L \underset{k_4}{\overset{k_3}{\rightleftharpoons}} R2\text{-}L$	$k_3 = 0.042 \pm 0.002\ s^{-1}$	Plateau value of the rate constant for the slow relaxation
	$k_4 = 0.005 \pm 0.002 s^{-1}$	Fitting of k_{app} for the slow relaxation
$R2\text{-}L \xrightarrow{k_5} R2 + L$	$k_5 = 0.005 \pm 0.001 s^{-1}$	Fitting of dissociation after equilibrium association is reached
$R1\text{-}L \xrightarrow{k_6} R1 + L$	$k_6 = 0.03 \pm 0.01\ s^{-1}$	Fitting of dissociation relaxation after short time TR1-NKA association

the short variant TR7-NKA-(4–10). This difference between the two agonists may correlate with the fact that only TR1-NKA appears to stabilize a "desensitized" conformation of the receptor. Associated with the difference in the mode of binding of the two agonist peptides and in agreement with previous observations made with NKA on tachykinin receptors (32, 33), we find that only the long agonist peptide is able to stimulate cAMP formation in a calcium-independent manner. The intracellular pathway leading to such rise in cAMP concentration is not identified in this work. It is, however, unlikely to result from direct activation of calcium-dependent adenylyl cyclases since (i) both agonists trigger intracellular calcium elevations of similar amplitude and (ii) chelation of calcium by BAPTA does not affect the cAMP response. The delay between ligand binding and cAMP response onset suggests indirect coupling between the receptor and adenylyl cyclase. Phospholipase A_2 has been suggested as a possible effector (34, 35), since its inhibitor quinacrine has been be shown to block cAMP formation. Further work should help determine which pathway is selectively activated by the long peptide and to establish a more precise temporal correlation between slow binding and cAMP responses.

A Multiple State Model—The kinetic analyses presented here support the notion that multiple affinity states are differentially populated by the two ligands. These multiple affinity states may correspond to distinct conformations endowed with specific pharmacological and functional properties, associated with specific rates of interconversion between discrete conformations. In order to describe the time course of ligand binding more completely, we applied a kinetic model of agonist binding based upon the capacity of the receptor to interconvert between a limited number of conformations that are differentially stabilized by ligands and correspond to distinct states of the receptor (29). The present modeling of the NK2 receptor is carried out as follows: (*a*) by assuming a linear cascade for the interconversion between states, (*b*) by using all kinetic parameters determined experimentally for each ligand (Table I), and (*c*) by imposing the condition that the parameters that are intrinsic to the receptor (equilibrium constants between states in the absence of ligand) are identical in the modeling of TR1-NKA and TR7-NKA-(4–10) binding (Fig. 6). We find that with all these constraints it is possible to describe the binding of the two agonists to the receptor with a unique set of equilibrium constants for the interconversion between a minimal number of three conformations, denoted R0, R1, and R2, and binding constants specific to each ligand.

The R0 state corresponds to a low affinity (K_D >100 nM) conformation that represents ~72% of the total receptor states in the absence of ligand (see legend to Fig. 6). Such low affinity values match those determined from competition experiments using the antagonist SR 48968 (this work and Ref. 36).

The R1 state corresponds to an intermediate state that results from interconversion of the R0 state at a rate of ~4.5 s^{-1}. This interconversion rate is faster than agonist binding (0.1 to 2 s^{-1}) and is not readily detected in association kinetics. The affinity of the R1 state for the two agonists is about 10-fold higher than that of the R0 state. Its fractional concentration in the absence of ligand is about 10%, in agreement with its natural abundance recently determined for 5HT4 receptors (37). Since the R0 state rapidly equilibrates with the R1 state, fast agonist binding, as monitored in rapid mixing experiments, reflects a combination of association with pre-existing molecules in the R0 conformation together with binding to molecules rapidly interconverting to the R1 state.

The R2 state corresponds to the apparently unique state that becomes stabilized at equilibrium by TR1-NKA but not by TR7-NKA-(4–10). Its rate of stabilization (~0.05 s^{-1}) is slower than the rate of ligand binding to the receptor (0.1 to 2 s^{-1}) and corresponds to the slow binding rate of TR1-NKA. The affinity of this conformation (in the nM range) for TR1-NKA is close to the ligand equilibrium affinity, and its fractional concentration in the absence of ligand is about 18%. Within this framework of conformational states, binding of the truncated agonist, TR7-NKA-(4–10), is accounted for by assuming that it exhibits moderate to low affinity for the R2 conformation (K_DR2 > K_DR1). The TR7-NKA-(4–10) equilibrium binding affinity is

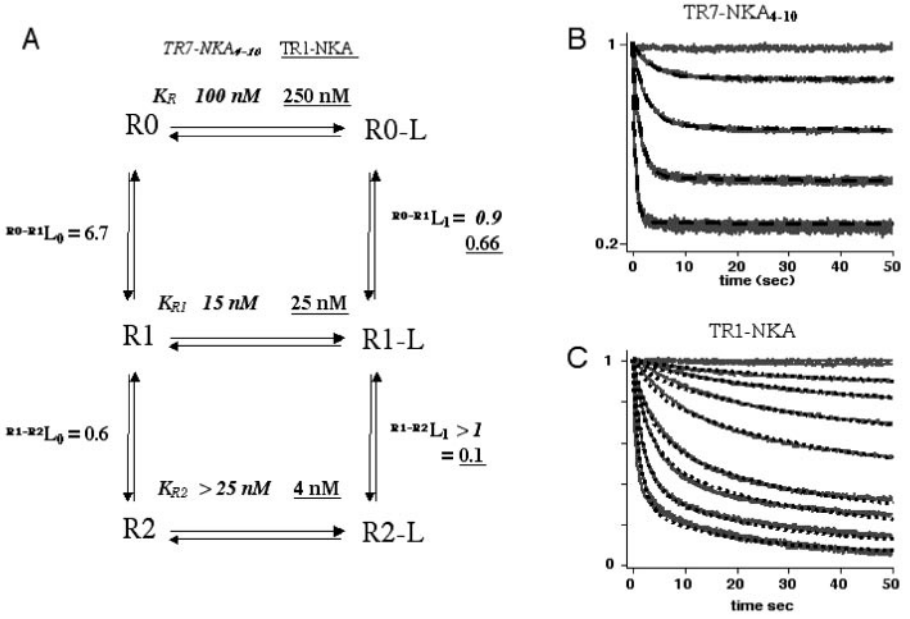

FIG. 6. **A three-state model (*A*) used to simulate binding kinetics of TR1-NKA (*B*) and TR7-NKA-(4–10) (*C*).** Intrinsic isomerization constants of the receptor in the absence of ligand are denoted L_0 ($^{R0\text{-}R1}L_0$ = [R0]/[R1]). Affinity constants K for the R0, R1, and R2 states are given for TR1-NKA (*underlined values*) and TR7-NKA-(4–10) (*italic values*). Isomerization constants of liganded conformations are given for each agonist as L_1 values ($^{R0\text{-}R1}L_1$ = [R0-*L*]/[R_1-*L*]) in *italics* (TR7-NKA-(4–10)) or *underlined* (TR1-NKA). Simulations were carried out using experimentally defined data given in Table I. Derived kinetic parameters were estimated by simultaneous manual fitting of binding traces for the two ligands and imposing identical L_0 values. Intrinsic rate for the R0 → R1 transition, 4.5 s^{-1}; intrinsic rate for the R1 → R0 transition, 30 s^{-1}; intrinsic rate for the R1 → R2 transition, 0.04 s^{-1}; and intrinsic rate for the R2 → R1 transition, 0.025 s^{-1}. Dissociation rate constant of TR1-NKA for the R0 state, 0.5 s^{-1}, and dissociation rate constant of TR7-NKA-(4–10) for the R2 state, >0.12 s^{-1}. The data, based on experiments shown in Figs. 1*A* and 2*A* are presented as *continuous curves,* and the simulations are shown as *dashed* (*B*) or *dotted* (*C*) *lines.* With the values obtained in simulation, the fractional distribution of the R0, R1, and R2 conformational states are R0 = 0.715; R1 = 0.107; and R2 = 0.178.

indeed close to that estimated for the R1 state.

The interconversion equilibrium constants used here to describe the receptor in the absence of ligand (L_0 values in Fig. 6*A*) are determined in a cellular environment, *i.e.* with all effectors of the response being present and functional. Phosphorylation events, or interactions with arrest proteins, which are clearly detected in functional assays and ligand binding kinetics, are therefore taken into account, but their contribution to the equilibria between conformations has not been explicitly determined. The L_0 values thus do not correspond to authentic intrinsic receptor interconversion constants and are expected to change with the cellular environment, *i.e.* at different receptor to effector ratios.

Functional Properties of the Multiple States—The observed correlation between the amplitude of rapid agonist binding and the onset of the calcium response supports the notion that the R1 state, which is in rapid equilibrium with the R0 state, represents an active conformation that triggers G_q protein activation. This active conformation is populated by the two agonists that both elicit IP_3 formation and calcium elevation.

The abundance of the R1 conformation in the absence of added agonist (see legend to Fig. 6) is in agreement with spontaneous activity of G protein-coupled receptors (37–40), detected *in vitro* and *in vivo*, and described as a basal activity reduced by inverse agonists (41–45). The rate of R1 state stabilization by the agonist, derived from receptor modeling, coincides with the rate of calcium response onset determined experimentally.

Based on kinetic arguments, there is apparent temporal correlation between slow TR1-NKA binding and cAMP-evoked responses. Indeed, slow binding develops on the time scale of tenths of seconds to minutes, and significant cAMP accumulation becomes detectable only after a delay of tenths of seconds at high agonist concentrations. Furthermore, in contrast to TR7-NKA-(4–10), only TR1-NKA exhibits slow binding and stimulates cAMP accumulation. The simplest interpretation of the experimental data therefore would be that transition toward the R2 state involves a second active state that couples to adenylate cyclase activation. Such an interpretation is supported by the earlier descriptions of dual calcium and cAMP responses mediated by different G proteins (1, 46–48) or dual activation and inhibition of adenylate cyclase by β-adrenergic receptors (1). However, the R2 state, as the conformation likely to become stabilized at equilibrium by TR1-NKA, may not itself represent a conformation that is active with respect to cAMP formation, since cAMP responses are known to desensitize (49), as do calcium responses. The conversion of a fraction of the receptor molecules from an active to an inactive conformation via a cAMP-stimulating conformation may occur without significant change in affinity of the receptor for TR1-NKA and could therefore remain undetectable in the present work.

Role of Protein Kinases and Possible Physiological Implications—The overall effects of protein kinase effectors support the notion that phosphorylation of the receptor differentially stabilizes conformations of the receptor (12, 50) by exhibiting conformation dependence in their specificity. Indeed, in agreement with the observed temporal correlation between rapid binding and activation of the calcium response, effectors of protein kinase C affect the intensity of the calcium response and the relative rapid/slow binding amplitudes (yet without changing the rates of rapid *versus* slow binding), whereas effectors of PKA (which have no effect on calcium responses) affect the rate of slow agonist binding but have no effect on the rate of rapid binding.

Following the calcium response and depending on the agonist used, an elevation of the intracellular cAMP concentration is detected. Interestingly, this cAMP response is potentiated or depressed when PKC is activated or inhibited, respectively. The cAMP elevation is also potentiated by inhibition of PKA, as expected for PKA being involved in the termination of the

cAMP response. Altogether these effects suggest that two distinct responses are mediated by different interconvertible functional states of the receptor and that phosphorylation by PKC should be viewed as a stop signal for a rapidly developing IP_3/calcium response and as a possible start signal for a slowly developing cAMP response. PKA may then become activated subsequent to the cAMP response and could in turn contribute to inactivation of this receptor-evoked signaling. Indeed, in terms of agonist binding kinetics, activators (*versus* inhibitors) of protein kinase A accelerate (*versus* slow down) the rate at which equilibrium is reached. Although the present data support the existence of two functional active states of the receptor separately leading to calcium and cAMP responses, they do not firmly establish a structural difference between the two states.

Such a dual phosphorylation process is supported by analyses of tachykinin receptor phosphorylation patterns showing qualitative differences in the distribution of phosphorylated residues when comparing activation of phosphorylation by phorbol esters (PMA) or by agonist (51). Furthermore, a particular phosphorylation pattern of the receptor may direct it toward further regulatory processes such as internalization and degradation or further signaling of other intracellular responses. Hence, NK1 (3) and NK2 (19) receptors stimulate, in an agonist-dependent manner, the MAP kinase cascade following interaction with arrestin.

Although tachykinin receptors do not mediate cAMP accumulation when expressed at low density in heterologous systems (33), phosphorylation by PKA may nevertheless contribute to the regulation of their state of activity. Indeed, different cell types may express receptors activating cAMP/PKA signaling pathways, together with tachykinin receptors. Activation of such receptors simultaneously or prior to tachykinin receptors may lead to PKA activation. The activated tachykinin receptor would then become a substrate for phosphorylation by PKA, with consequences that remain to be determined.

Conclusions—It is becoming increasingly well documented that, as in the case of conventional allosteric proteins (29, 52), G protein-coupled receptors adopt several conformational states, among which more than one active state can be detected (1, 50). Tachykinin NK2 receptors follow this scheme by adopting at least three (possibly four) distinct conformations corresponding to different structures with specific pharmacological and functional properties. Stabilization of the individual conformations may be promoted by pharmacological agents such as agonists and antagonists, as well as by covalent modifications, such as phosphorylation of the receptor protein. These conformations may spontaneously interconvert to give rise to a fraction of active conformations in the absence of added agonists and antagonists. Finally, at variance with ligand-gated ion channels, certain conformations may, at the same time, be active with respect to one given response and inactive (or desensitized) with respect to another response.

Acknowledgments—We thank C. A. Maggi and F. Pattus for critical comments and Olivier Schaad for adapting the STOIC computer program.

REFERENCES

1. Daaka, Y., Luttrell, L. M., and Lefkowitz, R. J. (1997) *Nature* **390,** 88–91
2. Daaka, Y., Luttrell, L. M., Ahn, S., Della Rocca, G. J., Ferguson, S. S., Caron, M. G., and Lefkowitz, R. J. (1998) *J. Biol. Chem.* **273,** 685–688
3. DeFea, K. A., Vaughn, Z. D., O'Bryan, E. M., Nishijima, D., Dery, O., and Bunnett, N. W. (2000) *Proc. Natl. Acad. Sci. U. S. A.* **97,** 11086–11091
4. Ikeda, S. R. (1996) *Nature* **380,** 255–258
5. Reuveny, E., Slesinger, P. A., Inglese, J., Morales, J. M., Iniguez-Lluhi, J. A., Lefkowitz, R. J., Bourne, H. R., Jan, Y. N., and Jan, L. Y. (1994) *Nature* **370,** 143–146
6. Bence, K., Ma, W., Kozasa, T., and Huang, X. Y. (1997) *Nature* **389,** 296–299
7. Dikic, I., Tokiwa, G., Lev, S., Courtneidge, S. A., and Schlessinger, J. (1996) *Nature* **383,** 547–550
8. Honda, Z., Takano, T., Hirose, N., Suzuki, T., Muto, A., Kume, S., Mikoshiba, K., Itoh, K., and Shimizu, T. (1995) *J. Biol. Chem.* **270,** 4840–4844
9. Pitcher, J. A., Freedman, N. J., and Lefkowitz, R. J. (1998) *Annu. Rev. Biochem.* **67,** 653–692
10. Whistler, J. L., Chuang, H. H., Chu, P., Jan, L. Y., and von Zastrow, M. (1999) *Neuron* **23,** 737–746
11. Roettger, B. F., Ghanekar, D., Rao, R., Toledo, C., Yingling, J., Pinon, D., and Miller, L. J. (1997) *Mol. Pharmacol.* **51,** 357–362
12. Thomas, W. G., Qian, H., Chang, C. S., and Karnik, S. (2000) *J. Biol. Chem.* **275,** 2893–2900
13. Leff, P., Scaramellini, C., Law, C., and McKechnie, K. (1997) *Trends Pharmacol. Sci.* **18,** 355–362
14. Lecci, A., Giuliani, S., Tramontana, M., Carini, F., and Maggi, C. A. (2000) *Neuropeptides* **34,** 303–313
15. Maggi, C. A., Catalioto, R. M., Criscuoli, M., Cucchi, P., Giuliani, S., Lecci, A., Lippi, A., Meini, S., Patacchini, R., Renzetti, A. R., Santicioli, P., Tramontana, M., Zagorodnyuk, V., and Giachetti, A. (1997) *Can. J. Physiol. Pharmacol.* **75,** 696–703
16. Mantyh, P. W., DeMaster, E., Malhotra, A., Ghilardi, J. R., Rogers, S. D., Mantyh, C. R., Liu, H., Basbaum, A. I., Vigna, S. R., Maggio, J. E., and Simone, D. (1995) *Science* **268,** 1629–1632
17. De Felipe, C., Herrero, J. F., O'Brien, J. A., Palmer, J. A., Doyle, C. A., Smith, A. J., Laird, J. M., Belmonte, C., Cervero, F., and Hunt, S. P. (1998) *Nature* **392,** 394–397
18. Murtra, P., Sheasby, A. M., Hunt, S. P., and De Felipe, C. (2000) *Nature* **405,** 180–183
19. Alblas, J., van Etten, I., and Moolenaar, W. H. (1996) *EMBO J.* **15,** 3351–3360
20. Sagan, S., Chassaing, G., Pradier, L., and Lavielle, S. (1996) *J. Pharmacol. Exp. Ther.* **276,** 1039–1048
21. Garcia, M., Sakamoto, K., Shigekawa, M., Nakanishi, S., and Ito, S. (1994) *Biochem. Pharmacol.* **48,** 1735–1741
22. Torrens, Y., Beaujouan, J. C., Saffroy, M., Glowinski, J., and Tence, M. (1998) *J. Neurochem.* **70,** 2091–2098
23. Vollmer, J. Y., Alix, P., Chollet, A., Takeda, K., and Galzi, J. L. (1999) *J. Biol. Chem.* **274,** 37915–37922
24. Theodorsson-Norheim, E., Jornvall, H., Andersson, M., Norheim, I., Oberg, K., and Jacobsson, G. (1987) *Eur. J. Biochem.* **166,** 693–697
25. Nemeth, K., and Chollet, A. (1995) *J. Biol. Chem.* **270,** 27601–27605
26. Heidmann, T., and Changeux, J. P. (1980) *Biochem. Biophys. Res. Commun.* **97,** 889–896
27. Horn, R., and Marty, A. (1988) *J. Gen. Physiol.* **92,** 145–159
28. Cailla, H. L., Racine-Weisbuch, M. S., and Delaage, M. A. (1973) *Anal. Biochem.* **56,** 394–407
29. Edelstein, S. J., Schaad, O., Henry, E., Bertrand, D., and Changeux, J. P. (1996) *Biol. Cybern.* **75,** 361–379
30. Neubig, R. R., and Sklar, L. A. (1993) *Mol. Pharmacol.* **43,** 734–740
31. Posner, R. G., Fay, S. P., Domalewski, M. D., and Sklar, L. A. (1994) *Mol. Pharmacol.* **45,** 65–73
32. Alblas, J., van Etten, I., Khanum, A., and Moolenaar, W. H. (1995) *J. Biol. Chem.* **270,** 8944–8951
33. Sagan, S., Karoyan, P., Chassaing, G., and Lavielle, S. (1999) *J. Biol. Chem.* **274,** 23770–23776
34. Arkinstall, S., Emergy, I., Church, D., Chollet, A., and Kawashima, E. (1994) *FEBS Lett.* **338,** 75–80
35. Catalioto, R. M., Cucchi, P., Renzetti, A. R., Criscuoli, M., and Maggi, C. A. (1998) *Naunyn-Schmiedeberg's Arch. Pharmacol.* **358,** 395–403
36. Huang, R. R., Vicario, P. P., Strader, C. D., and Fong, T. M. (1995) *Biochemistry* **34,** 10048–10055
37. Claeysen, S., Sebben, M., Becamel, C., Eglen, R. M., Clark, R. D., Bockaert, J., and Dumuis, A. (2000) *Mol. Pharmacol.* **58,** 136–144
38. Alewijnse, A. E., Timmerman, H., Jacobs, E. H., Smit, M. J., Roovers, E., Cotecchia, S., and Leurs, R. (2000) *Mol. Pharmacol.* **57,** 890–898
39. Kjelsberg, M. A., Cotecchia, S., Ostrowski, J., Caron, M. G., and Lefkowitz, R. J. (1992) *J. Biol. Chem.* **267,** 1430–1433
40. Lefkowitz, R. J., Cotecchia, S., Samama, P., and Costa, T. (1993) *Trends Pharmacol. Sci.* **14,** 303–307
41. Alewijnse, A. E., Smit, M. J., Hoffmann, M., Verzijl, D., Timmerman, H., and Leurs, R. (1998) *J. Neurochem.* **71,** 799–807
42. Charpentier, S., Jarvie, K. R., Severynse, D. M., Caron, M. G., and Tiberi, M. (1996) *J. Biol. Chem.* **271,** 28071–28076
43. Milano, C. A., Allen, L. F., Rockman, H. A., Dolber, P. C., McMinn, T. R., Chien, K. R., Johnson, T. D., Bond, R. A., and Lefkowitz, R. J. (1994) *Science* **264,** 582–586
44. Niswender, C. M., Copeland, S. C., Herrick-Davis, K., Emeson, R. B., and Sanders-Bush, E. (1999) *J. Biol. Chem.* **274,** 9472–9478
45. Parma, J., Van Sande, J., Swillens, S., Tonacchera, M., Dumont, J., and Vassart, G. (1995) *Mol. Endocrinol.* **9,** 725–733
46. Eguchi, S., Hirata, Y., Imai, T., and Marumo, F. (1993) *Endocrinology* **132,** 524–529
47. Pommier, B., Da Nascimento, S., Dumont, S., Bellier, B., Million, E., Garbay, C., Roques, B. P., and Noble, F. (1999) *J. Neurochem.* **73,** 281–288
48. Wang, L., Gantz, I., and DelValle, J. (1996) *Am. J. Physiol.* **271,** G613—G620
49. Lefkowitz, R. J. (1998) *J. Biol. Chem.* **273,** 18677–18680
50. Francesconi, A., and Duvoisin, R. M. (2000) *Proc. Natl. Acad. Sci. U. S. A.* **97,** 6185–6190
51. Roush, E. D., Warabi, K., and Kwatra, M. M. (1999) *Mol. Pharmacol.* **55,** 855–862
52. Galzi, J. L., Edelstein, S. J., and Changeux, J. (1996) *Proc. Natl. Acad. Sci. U. S. A.* **93,** 1853–1858